Nanoscale

Supplementary Information

Facile synthesis of WS_2 nanotubes by sulfurization of tungsten thin films: formation mechanism, structural and optical properties†

Emroj Hossain*[a], Azizur A Rahman[a], Rudheer D Bapat[a], Jayesh B Parmar[a], Amit P Shah[a], Ashish Arora[b], Rudolf Bratschitsch[b], Arnab Bhattacharya[a]

1 TEM sample preparation

Cross sectional TEM samples were prepared without an FIB using a novel process that provides cross sections of multiple nanotubes (NTs) at the same time. The WS_2 NTs are aligned vertically on the sapphire substrate on top of the thin film of WS_2. First Gatan G1 epoxy was put on top of the sample and hardened by heating. Since the WS_2 is attached to sapphire via weak van der Waals forces, the WS_2 layer along with nanotubes and epoxy is easily removed mechanically from the sapphire substrate. The epoxy with embedded NTs was mechanically polished from both sides to remove the underlying WS_2 layer while keeping the NTs intact. Dimpling was done from the top side using a dimple grinder. The sample was thinned down further by ion milling from both sides at 5^o angle with a 4 keV Ar^+ beam. When the sample was about to perforate the voltage was reduced to 2.5 keV for fine thickness control. The sample was then mounted on a TEM grid. Probe corrected STEM was performed using 300 keV TITAN microscope. High-angle annular dark-field imaging (HAADF) with resolution down to 0.7 Å was achievable.

2 SEM

Fig. 2 shows the SEM image of WS_2 sample grown at 950 ^oC near the critical temperature for the formation of nanotubes. The coexistance of horizontal and vertical WS_2 and the nanotubes can be seen in the magnified SEM image in Fig. 2.

3 AFM

Atomic force microscopy was done on the nanotube sample using PARK XE AFM in tapping mode over 250 nm$\times$ 250 nm. From the AFM image in Fig. 3 the length of the nanotubes is found to be $\sim$150 nm and outer diameter $\sim$ 30 nm. The diameter value is relatively larger than that found in TEM, partly because the NT diameter is convoluted with the AFM tip diameter.

* *E-mail: emroj.hossain@tifr.res.in; Tel: +91 22 2278 2517*

[a] *Tata Institute of Fundamental Research, Homi Bhabha Road, Colaba, Mumbai 400005, India*

[b] *Institute of Physics and Center for Nanotechnology, University of Münster, Wilhelm-Klemm-Str.10, 48149 Münster, Germany*

4 EDS

EDS measurement in TEM in Fig. 4 confirms the presence of tungsten and sulfur in WS_2 nanotubes.

5 XRD

Grazing angle XRD as shown in Fig. 5 was done for the nanotubes samples using a PANalytical powder XRD system. Horizontal WS_2 thin film is oriented along the c-direction. So in general, for thin film WS_2 only the peaks corresponding to (0 0 2) and its higher order planes is observed in powder XRD. For the NT sample the peak corresponding to (0 0 2) was observed at 14.2^o and the peak corresponding to (1 0 0) was observed at 33^o. Therefore, the peak corresponding to (1 0 0) was expected to originated from both NTs or vertically oriented flakes. The other peaks corresponding to (1 0 3) and (1 1 0) were also observed.

6 Determination of chiral indices for multi-walled nanotubes

Let's first consider the case of single-walled nanotubes (Fig. 6(a)). While taking the diffraction pattern the electron beam will pass through two layers of WS_2 i.e. top layer and bottom layer. Each layer contains a hexagonal arrangement of tungsten and sulfur atoms. Hence the diffraction pattern for each layer will have hexagonal spots. However, since the layers are not planar but curved these spots will spread out in the nanotube radial direction due to the curvature resulting in diffraction "lines". Now the top and bottom layer will give rise to a different set of hexagonal lines, which will, in general, not coincide if the nanotubes are chiral but will be rotated with each other (Fig.6(d)). The amount of rotation of the two diffraction patterns is related to the ratio of chiral indices (v/u). Now multi-walled nanotubes can be considered as concentric single-walled nanotubes [1,2]. For each wall, there will be two sets of layers and for each layer, there will be a set of hexagonal diffraction lines. So in general if there is a N walled (N=2 in Figs. 6(b)&(c)) chiral nanotube with each layer having different ratio of chiral indices (v/u), the electron beam will pass through 2N layers and as a result one would expect 2N

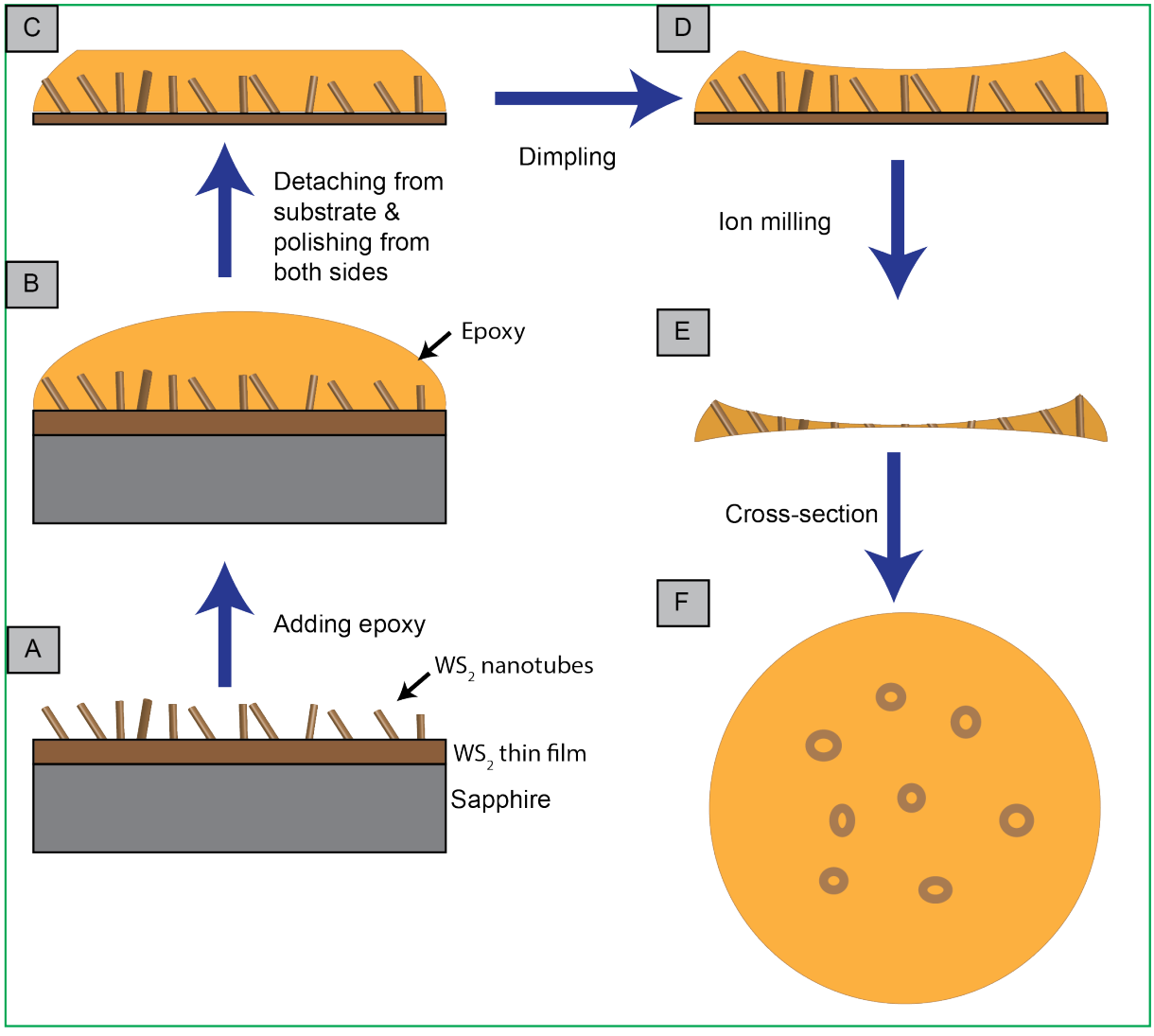

Fig. 1 Cross-sectional TEM sample preparation

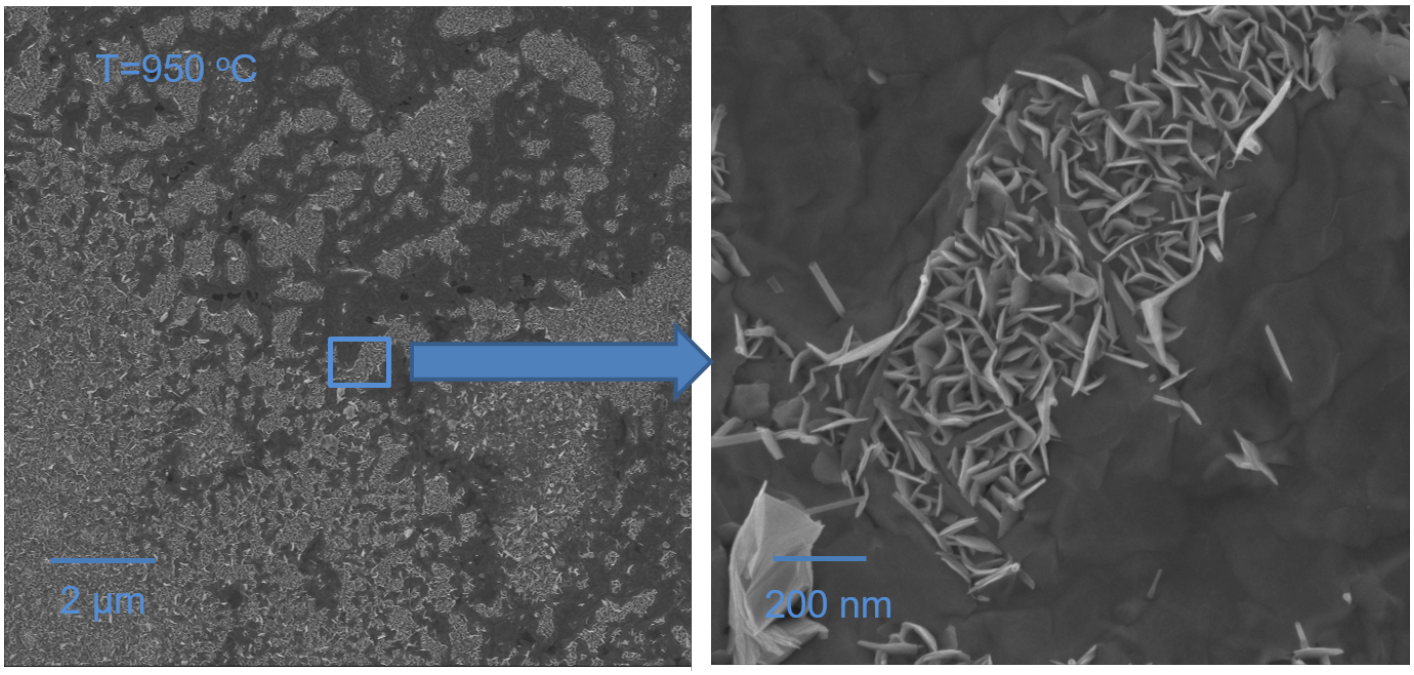

Fig. 2 SEM image highlighting the coexistance of vertical and horizontal morphology along with nanotubes

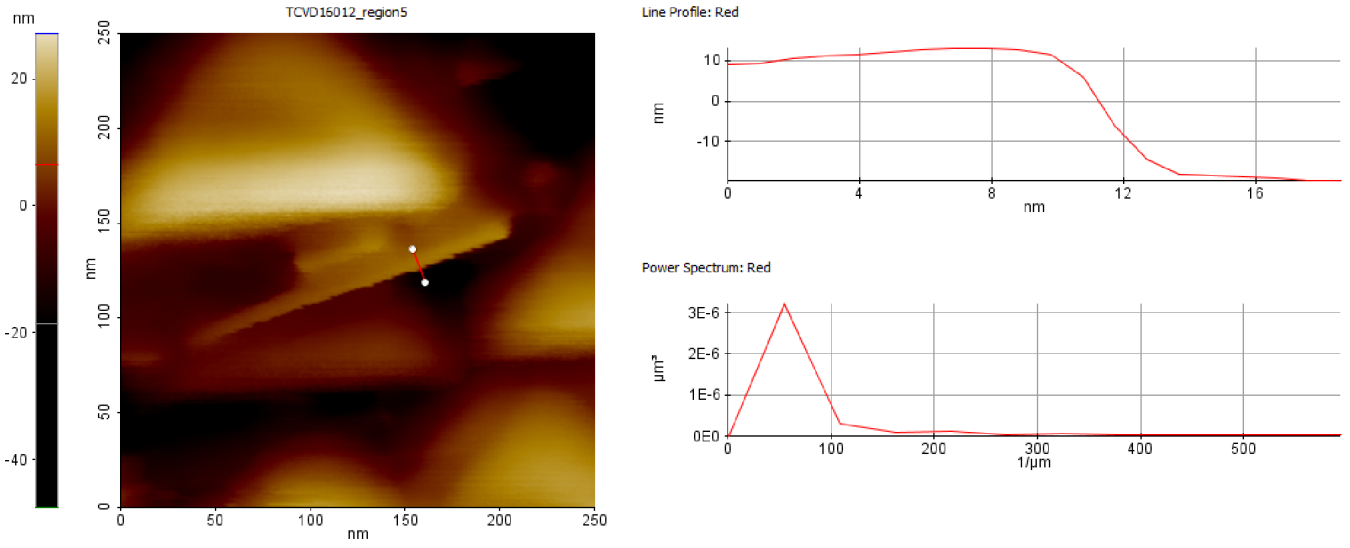

Fig. 3 AFM image of WS_2 nanotube

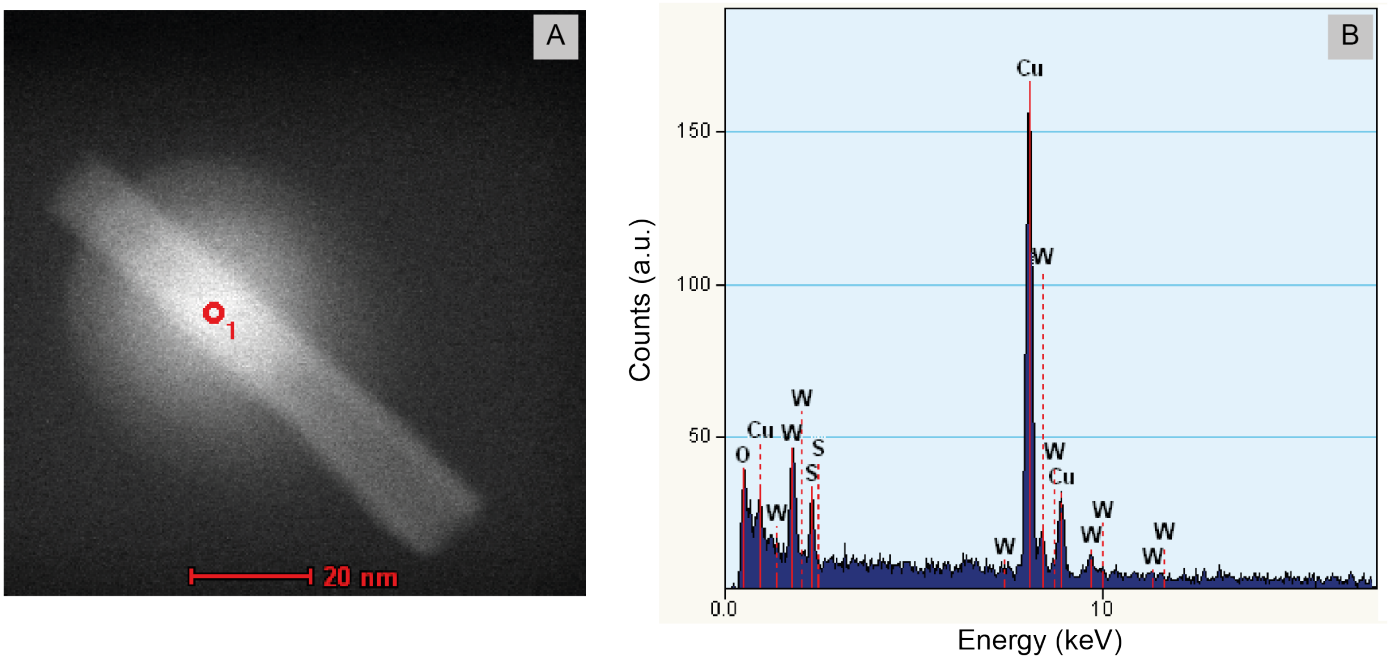

Fig. 4 (A)TEM image of the WS_2 NT. Point shows the region where EDS were done. (B) EDS quantification of WS_2 NT

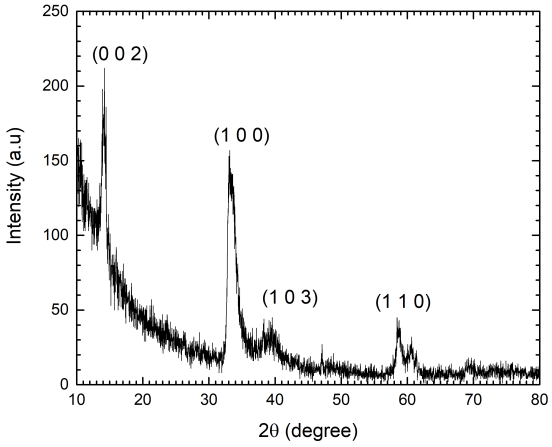

Fig. 5 Grazing angle XRD of the WS_2 nanotubes along with flakes

sets of diffraction patterns (Fig. 61(e)). However, if all the walls have the same chiral indices ratio (v/u) (Fig. 6(c)) these 2N sets of hexagonal patterns will overlap with each other and resulting in only two sets (corresponding to chirality) of hexagonal patterns (Fig. 6(f)).

In our case, in the diffraction pattern (FFT) shown in the main manuscript (Fig. 4(e)) we observe only two sets of hexagons. This diffraction pattern suggests that each wall of the nanotube has the same chiral indices ratio (v/u). This is also not surprising, since the nanotube was formed by the wrapping of a single flake, each layer of which was wrapped in the same way. So one would expect the same ratio of chiral indices for each wall. The absolute values of the chiral indices for each layer depend on the diameter of each wall. So by measuring the nanotube diameter for each wall from the TEM absolute values of the chiral indices for each wall were determined. Since the absolute value of the chiral indices depend on the diameter it can be different for each wall in spite of them having the same chiral indices ratio.

7 Analysis of transmission spectrum

The line shape of the transmission spectrum was modeled using a transfer matrix based approach in the 1.67 eV - 2.25 eV energy region, to take into account interference effects due to the nanoflakes and nanotubes on the sample surface[3]. As has been mentioned in the main text, the light scattering losses are neglected due to a much smaller average diameter of the nanotubes when compared to the wavelength of light. The wavelength-dependent complex refractive index $n_b + ik_b$ of WS_2 was used to represent the background dielectric function $\varepsilon_b = \beta(n_b + ik_b)^2$ of the sample, without the excitonic effects[4]. The multiplicative parameter $0<\beta<1$ considers the fact that the surface of the sample is perforated. The excitonic contribution to the dielectric function

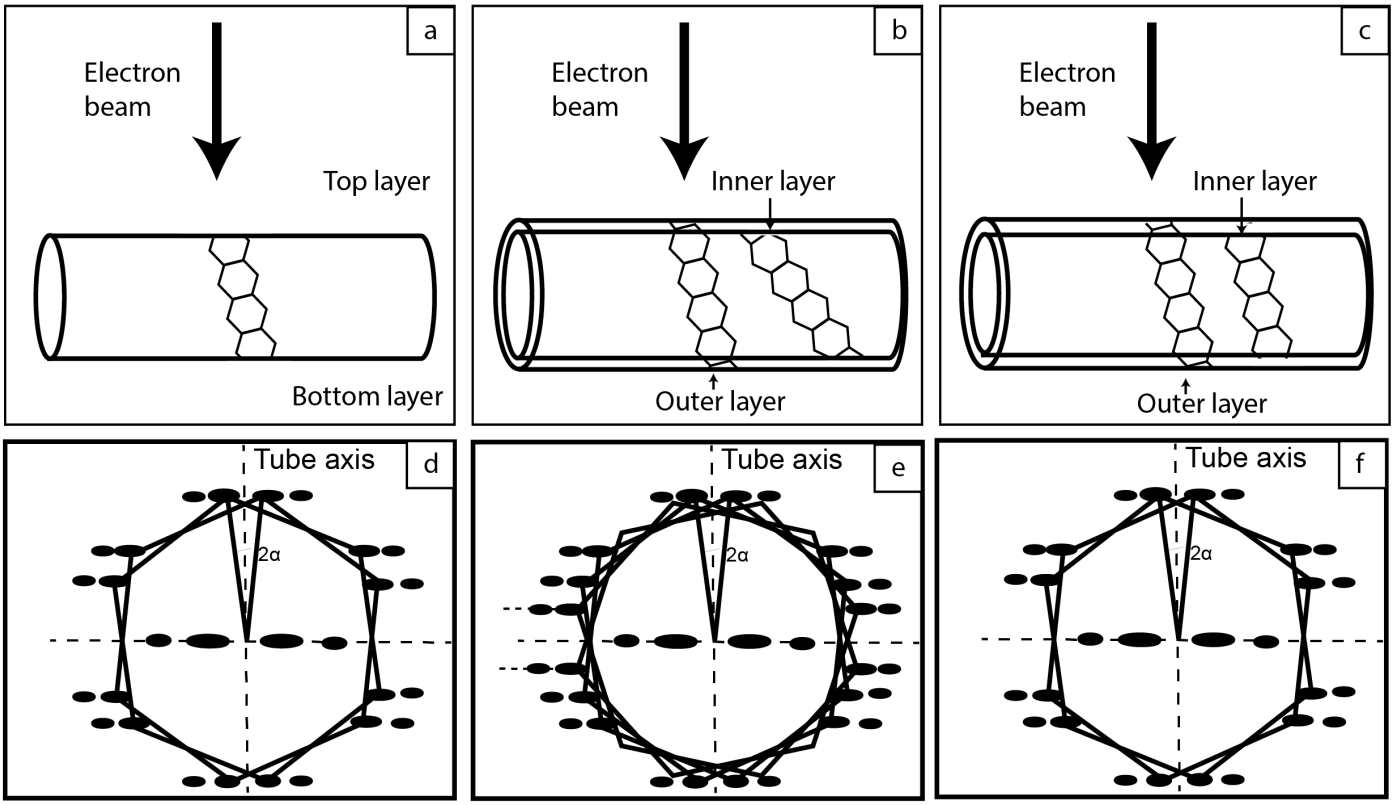

Fig. 6 Schematic diagram of (a) single walled, nanotube, (b) multi-walled nanotube with different chiral indices ratio and (c) multi-walled nanotube with same chiral indices ratio. (d), (e), (f) show the diffraction pattern corresponding to nanotubes shown in (a), (b), (c) respectively

was included by complex Lorentz oscillator functions[5]. Therefore, the overall dielectric function can be written as

$$\varepsilon(E) = \beta(n_b + ik_b)^2 + \sum_j \frac{A_j}{(E_{0j}^2 - E^2 - i\gamma_j E)} \quad (1)$$

whereA_j,E_{0j}, and γ_j are the oscillator strength, energy and the full-width at half-maximum respectively, of the j^{th} resonance. The best fit to the measured transmission spectrum (red curve in Fig. 5b in the main paper) was obtained for an effective WS_2 thickness of 25 nm and $\beta = 0.7$.

Notes and references

1 C. S. Allen, C. Zhang, G. Burnell, A. P. Brown, J. Robertson and B. J. Hickey, *Carbon*, 2011, **49**, 4961–4971.

2 H. Deniz and L.-C. Qin, *Chemical Physics Letters*, 2012, **552**, 92–96.

3 E. Hecht, *Optics*, Pearson, 2015.

4 Y. Li, A. Chernikov, X. Zhang, A. Rigosi, H. M. Hill, A. M. van der Zande, D. A. Chenet, E.-M. Shih, J. Hone and T. F. Heinz, *Physical Review B*, 2014, **90**, 205422.

5 A. Arora, A. Mandal, S. Chakrabarti and S. Ghosh, *Journal of Applied Physics*, 2013, **113**, 213505.